Interface chemistry and epitaxial growth modes of SrF_2 on Si(001)

L. Pasquali,[1] S. M. Suturin,[2] A. K. Kaveev,[2] V. P. Ulin,[2] N. S. Sokolov,[2] B. P. Doyle,[3] and S. Nannarone[1,3]
[1]*Dipartimento di Ingegneria dei Materiali e dell'Ambiente, Università di Modena e Reggio Emilia, Via Vignolese 905, 41100-Modena, Italy*
[2]*RAS, Solid State Optics Department, Ioffe Physical-Technical Institute, 26 Polytechnicheskaya, 194021 St. Petersburg, Russia*
[3]*INFM-CNR-TASC Laboratory, s.s. 14, km 163.5 in AREA Science Park, 34012 Basovizza (TS), Italy*
(Received 2 October 2006; revised manuscript received 13 December 2006; published 2 February 2007)

Molecular beam epitaxy has been used to grow SrF_2 thin films on Si(001). The growth modes have been investigated by atomic force microscopy, electron diffraction, and photoemission. Two principal growth regimes have been identified: (i) when deposition is carried out with the substrate held at a temperature of 700–750 °C, SrF_2 molecules react with the substrate giving rise to a Sr-rich wetting layer on top of which three dimensional bulklike fluoride ridges develop; (ii) when deposition is carried out with the substrate held at 400 °C, a nanopatterned film forms with characteristic triangular islands. Results are compared to the growth mode of CaF_2 on Si(001) under analogous deposition conditions. Morphological and structural differences between the two systems are associated with the larger lattice parameter of SrF_2 with respect to CaF_2, resulting in a larger mismatch with the Si substrate.

DOI: 10.1103/PhysRevB.75.075403 PACS number(s): 61.14.Hg, 68.37.Ps, 73.90.+f, 79.60.Jv

I. INTRODUCTION

The study of the growth of insulators on semiconductors is an attractive field both for fundamental research and technological applications. In particular, the formation of interfaces between different materials and the Si(001) surface, which is the most relevant for technological applications, usually results in three-dimensional (3D) structures whose morphology, crystal structure, and size critically depend on the suitable choice of the growth parameters (substrate temperature, substrate orientation, deposition method, etc.) The growth mode and film morphology can thus be tailored through the knowledge and control of the growth parameters, with the possibility to tune the film quality and properties.

We recently investigated the growth mode of CaF_2 on Si(001) by molecular beam epitaxy (MBE) at different substrate temperatures during deposition.[1–4] It was found that at low coverage and at low temperature of deposition, i.e., 400–500 °C, rectangular shaped CaF_2 nanoscale islands develop, leaving portions of the Si surface unreacted in between the islands. The fluoride islands are uniformly distributed over the surface and grow with their [001] axis aligned with the [001] axis of the substrate.

At deposition temperatures of 700–750 °C, CaF_2 molecules adsorbed at the surface dissociate, reacting and bonding to the silicon substrate atoms. Strong bonds are formed between the Si surface atoms and the Ca atoms in CaF dissociated species.[4] It was observed that the dissociative reaction takes place preferentially at the step edges of the Si substrate, with the consumption of Si atoms from the terrace edge. Due to the inequivalence of the step edges with respect to the orientation of the dimer chains of the Si(001) 2×1 reconstructed surface at different terrace edges,[5] certain terraces present an enhanced reactivity and are consumed preferentially. This produces a progressive transition from the double domain structure of Si(001) 2×1 to a twofold single domain structure once all the surface has been covered by a uniform reacted fluoride layer which "wets" the substrate surface.[4] The dissociative reaction appears to terminate at 1 ML of coverage. After this stage elongated islands (stripes) develop on top of the wetting layer running along either the [110] or $[1\bar{1}0]$ substrate directions. It was found that in this case the fluoride islands grow with their [110] axis aligned parallel to the [001] axis of the substrate.

The physical properties of strontium fluoride (SrF_2) are in many respects similar to those of CaF_2: both materials have the same fluorite-type crystal structure and show good insulating properties typical of wide band-gap materials. Epitaxial layers and nanostructures of strontium and calcium fluorides are interesting for basic studies of low dimensional effects and, doped with rare-earth ions, are quite attractive for applications in optoelectronics.[6] Moreover, the heteroepitaxial growth of fluorides has recently received considerable attention for possible applications in silicon based resonant tunneling devices.[7,8] Because of the formation of sharp and stable interfaces, fluorides could also find interesting applications as buffer layers in ultrathin semiconductor-insulator systems based on wide gap materials such as rare-earth oxides, preventing the oxidation of the semiconductor substrate.

Strontium fluoride has a considerably higher lattice parameter (5.80 Å) than calcium fluoride (5.46 Å) and silicon (5.43 Å); therefore a noticeable influence of the strain on the initial stages of growth and on the formation of the interface is expected.

This work aims at extending the study of the growth mode of cubic difluorides on Si(001) initiated with CaF_2, with the investigation of the formation of the SrF_2/Si(001) interface. To this end, the same experimental procedures adopted for the study of CaF_2 on Si(001) were followed.[4] In particular, SrF_2 was deposited in ultrahigh vacuum by MBE, at various substrate temperatures during deposition. Structural and morphological information were obtained by atomic force microscopy (AFM) and by *in situ* reflection high energy electron diffraction (RHEED). Low energy electron diffraction (LEED) was also used, supporting and confirming the

 ©2007 The American Physical Society

RHEED observations. Electronic properties were probed by x-ray and ultraviolet photoemission.

The results indicate that there exist strong similarities, but also considerable differences, between the growth modes of SrF_2 and CaF_2 on Si(001). The differences are mainly ascribed to the differences in the lattice parameters of CaF_2 and SrF_2 with respect to Si.

In particular it was observed that a dissociative reaction of SrF_2 takes place at high temperature, 700–750 °C, resulting in a uniform layer wetting the semiconductor surface and a strong bonding between the fluoride molecules and Si atoms. Similarly to the CaF_2 case, the deposition of subsequent layers induces the formation of elongated facetted islands (ridges). However, unlike almost one-dimensional CaF_2 ridges with typical sizes of (width $\times$ length $\times$ height) 10 nm $\times$ 1–3 μm $\times$ 10 nm, the SrF_2 ridges are more bulklike having typical sizes of 150 nm $\times$ 1 μm $\times$ 50 nm. In addition, the SrF_2 ridges have slightly different epitaxial relations to the Si substrate. At low deposition temperature below 500 °C, SrF_2 does not wet the Si surface and triangular shaped fluoride islands are formed from the earliest stages of deposition.

II. EXPERIMENT

The characterization of the growth mode of SrF_2 on Si(001) was carried out in separate experimental runs. Morphological and structural studies were carried out principally at the Ioffe Physical-Technical Institute (St. Petersburg, Russia) by AFM and RHEED. LEED and photoemission studies were conducted in part on-campus at the University of Modena and Reggio Emilia (Italy), and in part at the BEAR (BL 8.1L)[9] beam line at the ELETTRA synchrotron radiation facility (Trieste, Italy). The same growth conditions were employed both at the Ioffe and during photoelectron spectroscopy measurements, where the electronic properties of the system were studied.

In both cases $SrF_2/Si(001)$ samples were grown by MBE in UHV conditions at a pressure below 1×10^{-7} Pa. Deposition of strontium fluoride was made using a home built effusion cell, consisting of a graphite crucible loaded with small pieces of SrF_2 crystals. The crucible was heated by a tungsten grid filament up to about 1100 °C to produce a SrF_2 molecular beam. Due to strong ionic bonding, SrF_2 is known to sublime in the form of molecules, thus providing the stoichiometry of the beam.[10] The flux was calibrated by observing RHEED specular beam oscillations during the first stages of SrF_2 growth on a Si(111) substrate (at the Ioffe) or with a quartz micro balance (at BEAR and in Modena). The typical flux values used were in the range of 1–7 monolayers per minute [nominal monolayer—ML—corresponding to 2.9 Å of thickness on Si(001)]. Unless otherwise indicated, the growth rate employed for the samples used in the spectroscopic investigation was 1 nominal ML per minute.

Silicon substrate heating was provided either by indirect heating, passing electric current through a heater filament located closely behind the substrate (Ioffe, BEAR), or by direct heating, passing current through the substrate itself (Modena). The substrate temperature was monitored with an optical or IR pyrometer and additionally with a tungsten-rhenium thermocouple (Ioffe).

Si(001) *n*-type substrates were used with a miscut angle of 1–3 mrad with respect to the (001) plane. They were cleaned prior to the SrF_2 deposition, the procedure consisting of a standard chemical Shiraki treatment,[11] followed by flashing the surface up to 1100–1200 °C in UHV conditions to remove the silicon oxide.

The epitaxial relations and surface periodicity were monitored at Ioffe during sample growth with a RHEED apparatus (15 keV electron gun) mounted on the MBE chamber. LEED was used to monitor the surface periodicity during photoemission experiments (BEAR and Modena). Since RHEED and LEED data were in most cases complementary in what concerns surface periodicity, here we will present mainly RHEED data, which are also particularly powerful to show the lattice periodicity in the plane perpendicular to the surface. The latter can be obtained only when 3D islands develop at the surface. These are passed through by the *e* beam at grazing incidence leading to typical 3D diffraction patterns (transmission spots).

When electron diffraction measurements were performed on the same samples investigated by photoemission, diffraction patterns were always taken after the spectroscopy session, not to damage the interface or alter the surface composition, e.g., by preferential *F* removal induced by electron irradiation.[12]

Surface morphology of the grown samples was measured in tapping (semicontact) mode with an ambient air P4-SPM NT-MDT atomic force microscope equipped with NSCS-11 cantilevers having a resonance frequency of 200–300 kHz. Typical resolution of the AFM was 10–20 nm laterally and 1–2 Å in the direction of the surface normal, depending on the sharpness of the cantilever tip.

Photoemission spectra were recorded at BEAR with an hemispherical electron analyzer[13] at normal emission (with an angular acceptance of 2°). Ultraviolet and conventional x-ray photoemission data were recorded with a double pass Perkin Elmer PHI 15-255G cylindrical-mirror electron analyzer (CMA) operated at constant pass energy (Modena). The axis of the CMA was set to 15° from the sample normal. The energy resolution used varied according to the different spectral ranges investigated and type of experiment (synchrotron or on-campus). UV spectra (He I photons) were obtained with a windowless differentially pumped Vacuum Generators UV discharge lamp. X-ray photoemission was carried out with nonmonochromatic Mg $K\alpha$ photons ($h\nu$=1253.6 eV) from a Vacuum Generators XR3 dual anode source operated at 15 kV, 16 mA.

All spectra were measured at room temperature, letting the samples cool down for a few minutes after the deposition step. The spectra are reported in binding energy, referenced to the Fermi level position.

III. RESULTS AND DISCUSSION

A. Structure and morphology

1. Clean Si(001) surface

In order to understand the mechanisms of SrF_2 chemisorption as a function of temperature, a careful characteriza-

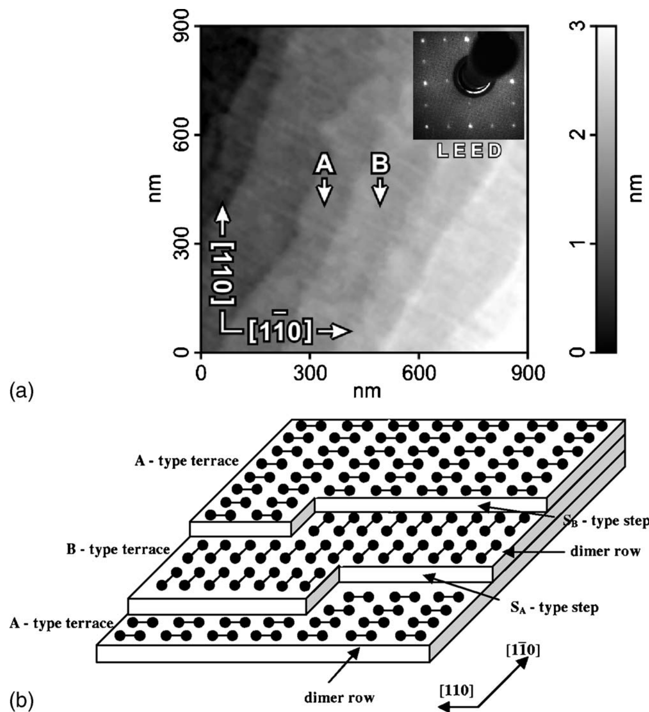

FIG. 1. (a) AFM image of the clean Si(001) surface. The typical LEED pattern due to the 2×1 double domain reconstruction is shown in the inset (electron beam energy $E_p=70$ eV). A and B indicate different terraces with perpendicular dimer row directions separated by single atomic steps. (b) Sketch of the clean Si(001) surface with dimer rows and steps.

tion of the bare Si(001) surface is mandatory. In the present study, Si(001) surfaces with a miscut angle of 1–3 mrad were chosen. This results in the formation of a stepped surface, where all terraces are separated by single atomic steps and run parallel to each other.[4] The terraces are characterized by alternate 2×1 and 1×2 reconstructions. This is due to the formation of dimers between adjacent Si surface atoms.[14] The surface morphology is illustrated in Fig. 1(a), where an AFM picture of the Si clean surface is shown. The AFM resolution does not allow the details of the surface reconstruction to be distinguished, but the alternation of the terraces can be observed clearly. The different terraces have been labeled by A and B consistently with Ref. 4. Each terrace is 50–150 nm wide and is separated from the adjacent one by single atomic steps of 1.4 Å in height, in agreement with the Si interlayer spacing along the [001] direction.

In complete analogy to our previous study on the growth mode of CaF_2 on Si(001),[4] we identify the [110] direction of the substrate as the one which forms an angle less than 45° with respect to the direction of the parallel step edges. Due to the relative orientation of the terraces and the Si crystallographic directions, it results that each step edge is characterized by longer segments parallel to the [110] directions than to the perpendicular [1$\bar{1}$0] direction. This situation is sketched in Fig. 1(b). From Fig. 1(b) it can be also noticed that adjacent terraces present different types of steps which run parallel to the [110] direction. These have been labeled as S_A-type and S_B-type according to the notation introduced by Chadi.[15] The nonequivalence of the steps depends on whether the dimer rows in the upper terrace are parallel (S_A-type) or perpendicular (S_B-type) to the step edge. As a consequence, the atomic structure around the step edges is locally perturbed, determining a variation of the dimer bucking asymmetry in correspondence with S_A-type steps[16,17] and a reorganization of the atoms at S_B-type steps. In particular, S_B-type steps present both a "nonrebonded" configuration and a "rebonded" one,[5,18] which is energetically favored and where Si edge atoms form dimerlike bonds with the lower terrace atoms.

It was shown for CaF_2[4] and we believe that this holds also for SrF_2 (see below), that the nonequivalence of the step edges plays an essential role in the determination of a single direction anisotropy of the fluoride interface layer during high temperature growth. We think that this is deeply related to the different and peculiar electronic structures of the two types of steps.

2. High-temperature growth

When SrF_2 is grown with the substrate held in the temperature range of 700–750 °C [Fig. 2(a)], thin nanostripes are formed. These nanostripes are less than 10 nm in width (our observation is limited by the resolution of the AFM) and they develop parallel either to the [110] or [1$\bar{1}$0] substrate directions depending on the type of Si terrace on which they grow. Stemming from the comparison with the CaF_2/Si(001) system,[4] each nanostripe is likely formed by fluoride molecules reacting with the substrate atoms. This conclusion is confirmed by our photoemission results (see below). Nanostripes are parallel to the [110] direction on B-type terraces and they are parallel to the [1$\bar{1}$0] direction on A-type terraces. This can be interpreted assuming that the growth direction is favored by the preferential diffusion of the admolecules along the direction of the dimer rows on each terrace, in agreement with observations on CaF_2/Si(001) (Ref. 4) and on alkaline-earth metals on Si(001).[19] The formation of the fluoride nanostripes is also accompanied by the progressive reorganization of the Si substrate terrace edges. With respect to this, the behavior of A and B-type terraces appears to be different. It can be seen in Fig. 2(a) that while B-type terraces present rather straight and uniform down-the-step edges, A-type terraces terminate at their down-the-step side with quite irregular and jagged profiles.

Although the effect is not well pronounced in Fig. 2(a), on the basis of the comparison with the CaF_2/Si(001) case and considering the uniaxial growth mode (see below), we infer that a preferential consumption of A-type terraces over B-type takes place. It was observed that while fluoride molecules do not modify the terrace in the down-the-step direction, the stripes develop at the expense of the upper terrace Si atoms, with the erosion of the edge itself. This means that each nanostripe grows consuming material from the upper terrace and that the active sites for nanostripe formation are located at the step edges. This also justifies the irregular profiles of A-type terraces at their down-the-step side [Fig. 2(a)].

The reason for the preferential consumption of A-type terraces is twofold. On the one hand, fluoride molecules spend

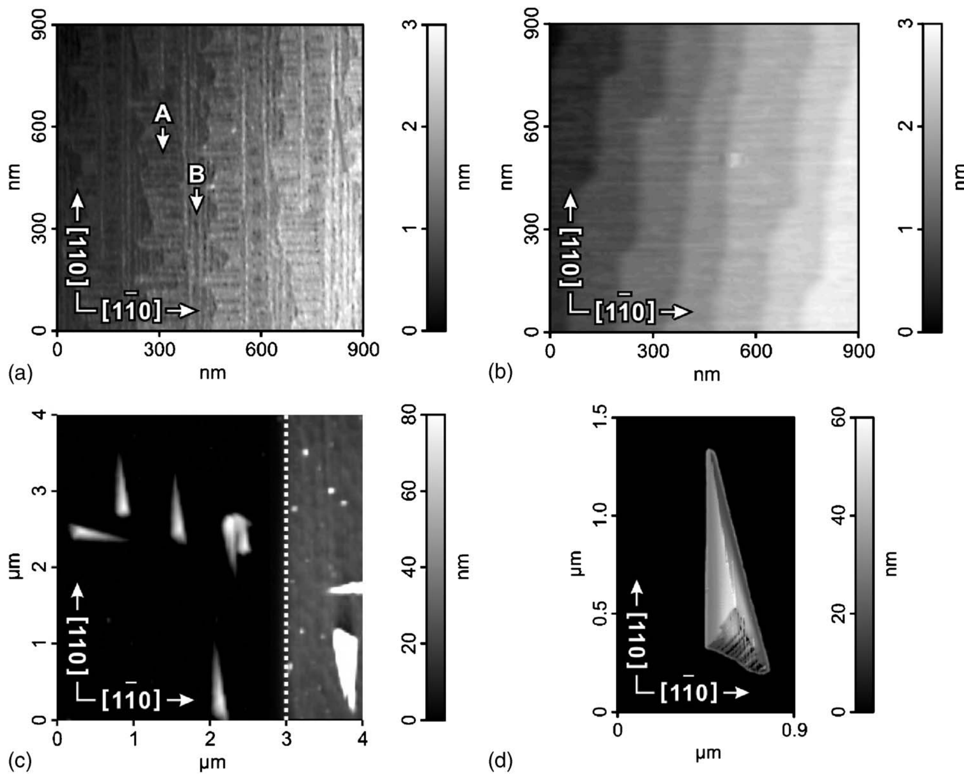

FIG. 2. AFM images of SrF_2 grown on Si(001) at 750 °C: (a) coverage 0.5 monolayer, (b) coverage 2 ML, (c) coverage 5 ML—widely separated ridges (the inset on the right highlights the flat area at the foot of the ridges) (d) coverage 5 ML individual ridge shown in greater detail.

a longer time over *B*-type terraces while diffusing along dimer rows with respect to *A*-type terraces. This enhances the nucleation probability of the stripes over *B*-type terraces, while the molecules tend to leave more easily *A*-type terraces when they reach the step edge with the lower terrace. On the other hand, the erosive reaction due to the fluoride molecules at high temperature at the step edges is expected to be decidedly different at S_B and S_A-type steps. This is because of the different structure (also in terms of local density of states and charge distribution) of the two types of steps. It should be noted that because of the relative terrace edges' orientations with respect to the Si crystallographic axes, *A*-type terraces present longer segments of S_B-type steps at the edge with the lower *B*-type terraces [see Fig. 1(b)]. The opposite occurs for *B*-type terraces. Our observations indicate that S_B-type steps are more active than S_A-type steps as far as the reactive nanostripe formation is concerned.[4] A reduction of the surface states energy gap was observed by scanning tunneling spectroscopy in correspondence to S_B-type steps,[20] suggesting the preferential evaporation and chemical etching of these sites with respect to S_A-type steps. This effect can also explain the behavior of the fluoride nanostripe formation in the present case.

In analogy to the CaF_2 case,[4] at about 1 ML of SrF_2 coverage, the single nanostripes coalesce to form a continuous layer, covering the surface uniformly [Fig. 2(b)]. This film is called the "wetting layer," in agreement with Ref. 4. The surface presents atomically flat terraces which are separated by steps of ~3 Å in height [note that the terrace width and step height are twice those of the clean Si(001) surface]. At this stage, *A*-type terraces are completely consumed and only *B*-type terraces survive, covered by the fluoride film. Because of this, the surface shows a clear single-axis anisotropy. This anisotropy is induced by the orientation of the stripes over *B*-type terraces. In Fig. 3, RHEED patterns taken with the *e*-beam parallel to the [110] direction are reported at different degrees of coverage. The typical 2×1 diffraction pattern of the clean Si(001) surface, with integer and half order spots appearing on the diffraction arc [Fig. 3(a)] is progressively substituted by a 3×1 periodicity [Fig. 3(b)] in the coverage range between 0.5 and 2 ML. This observation is confirmed by LEED. The same periodicity was also observed for CaF_2 deposited at high temperature.[4] With the electron beam along the [1$\bar{1}$0] direction (not shown), a reconstruction is observed with arcs following a 1/3 periodicity, consistent with the observations along the [110] direc-

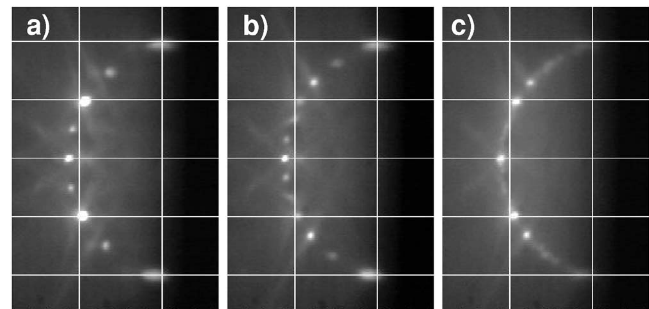

FIG. 3. RHEED patterns taken with the *e*-beam parallel to the [110] direction. (a) Clean Si(001) surface, the 2×1 reconstruction is visible. The grid lines are used as a guide of the eye to identify the integer order spots of the 1×1 surface. (b) Pattern corresponding to 0.5–2 ML of SrF_2 deposited at a substrate temperature of 750 °C. A 3×1 pattern substitutes the 2×1 of the clean surface. (c) Above 2 ML a 1×1 on-the-arc periodicity is superimposed onto blurred $1/N$ spots.

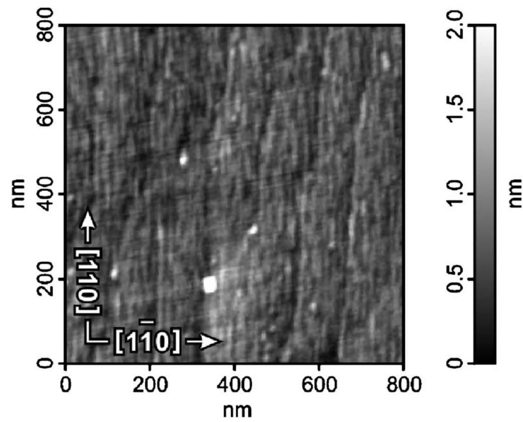

FIG. 4. AFM image taken on a film of 3 ML of SrF_2 grown at 400 °C over a film of 3 ML grown at 750 °C.

tion. The on-the-arc-periodicity is 1 or 1/2 depending on coverage.

With increasing fluoride coverage, in the range from 2 to 20 ML, three dimensional islands nucleate on top of the interface layer [Fig. 2(c)] with a typical density of one island per 1–5 square microns. From the fact that the growth of fluorides on Si leads to sharp and not intermixed interfaces,[21] from the comparison with previous work[4] and from our photoemission analysis (reported below) it can be concluded that the islands are formed by small SrF_2 crystallites. The islands have typical dimensions of ~50 nm in height, ~150 nm in width, and ~1000 nm in length. Each island has the shape of a ridge [Fig. 2(d)] that is formed by two facets: the steeper one inclined ~50° and the other one ~27° with respect to the substrate surface as measured from the AFM images. This makes ~103° between the planes. These facets seem to correspond to two SrF_2{111} planes intersecting at the ridge top, which is oriented along the SrF_2[001] direction and is almost parallel to Si[110]. This implies that the SrF_2[110] axis must be almost normal to the Si(001) surface. These epitaxial relations are similar to the case of CaF_2 on Si(001) at high temperature. It is worth noting that while in CaF_2 ridges the CaF_2[110] axis is strictly parallel to Si[001], for SrF_2 there is a misalignment angle of a few degrees between these directions.

Diffraction patterns obtained by RHEED [Fig. 3(c)] indicate an increased surface periodicity along the [1$\bar{1}$0] direction. With the *e*-beam along the [110] direction the on-the-arc-periodicity becomes $1/N$. The increase of the surface periodicity can be due to the large lattice mismatch between SrF_2 and Si. At the same time the elongated shape of the nanostripe which develops on top of the fluoride wetting layer accounts for the widening of the reflections in the direction of the increased periodicity, resulting in a coalescence of the reflections into streaks. It is worth noting that a similar behavior was observed recently for CaF_2 on Si(001).[22]

The single-axis anisotropic nature of the fluoride film is emphasized and can be evidenced also by the AFM if a few layers of SrF_2 are grown at low temperature over a film prepared at high temperature. This is shown in Fig. 4, where an AFM image of a film of 3 ML grown at low temperature (400 °C) over a film of 3 ML deposited at high temperature (750 °C) is presented. It can be clearly seen that low temperature growth leads to the formation of elongated islands over the high temperature grown film. These islands all appear parallel to each other and to the [110] direction of the Si substrate. Parallel terraces due to the substrate miscut are also well distinguishable. Since the growth mode of the low temperature film is driven by the geometrical properties of the supporting layer, this clearly indicates the single domain and twofold symmetry of the high temperature film.

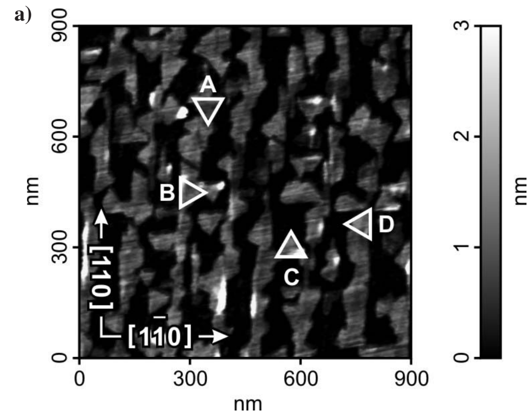

b)

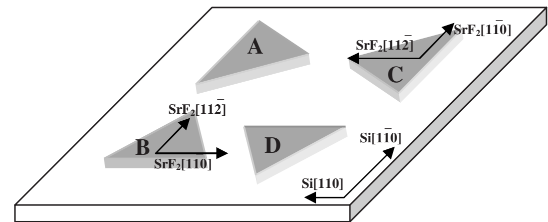

FIG. 5. (a) AFM image taken at 3 ML of SrF_2 coverage with the substrate held at 400 °C during growth. (b) Sketch of the orientation of the SrF_2 islands with respect to the Si(001) substrate plane.

3. Low-temperature growth

When SrF_2 is deposited at T=400 °C, flat triangular islands form on the Si surface. In Fig. 5(a) the surface morphology of a film of 3 ML of nominal coverage is reported as obtained by AFM. The islands appear to be rather uniform both in height (few MLs) and in lateral dimensions (30–40 nm). It can be seen that the islands do not cover the surface uniformly. RHEED, LEED, and spectroscopic data (see below) suggest that the area in between the islands remains clean silicon, in analogy to the growth of CaF_2 at the same temperature,[4] and that the islands are SrF_2 in composition. The SrF_2 nanostructures nucleate preferentially at the step edges of the Si substrate (step nucleation), tending to form long chains of partially coalesced islands which run parallel to the terrace edges. No apparent preferential nucleation at S_B or S_A type steps is observed. The triangular shape of the islands suggests that the SrF_2 lattice is oriented with its [111] axis perpendicular to the surface plane. This is consistent with the fact that (111)-oriented surfaces in fluorides present the lowest surface energy with respect to the other

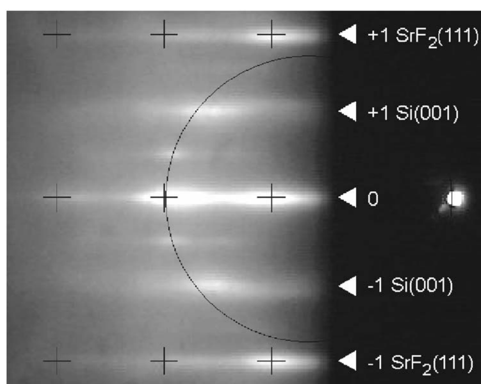

FIG. 6. RHEED pattern taken with the e-beam parallel to the Si[110] direction at 3 ML grown at 400 °C. The circle serves as a guide for the eye to recognize the 2×1 periodicity from the clean Si surface areas. Three-dimensional transmission spots are indicated by crosses.

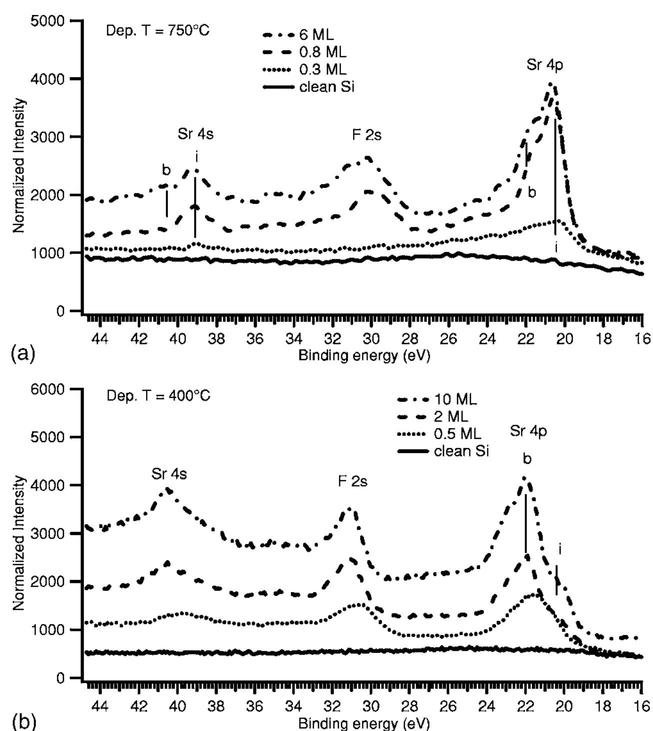

FIG. 7. Photoemission spectra recorded at a photon energy of 90 eV and at normal emission as a function of coverage with the substrate held at 750 °C (a) and 400 °C (b) during deposition.

high symmetry crystal faces.[21] Because of this, fluoride films tend to grow preferentially along the [111] direction and present (111) oriented facets.[4]

The SrF_2 triangular nanostructures present two different orientations rotated by 90° with respect to each other, corresponding in Fig. 5(a) to islands of type *A* and *C* and islands of type *B* and *D*. This is not unexpected and is related to the two possibilities to arrange the triangular (111) surface lattice of SrF_2 on the square (001) lattice of the substrate. This is schematically shown in Fig. 5(b): the triangular nanostructures present lateral edges which are parallel to the $[1\bar{1}0]$ direction of the fluoride lattice and may be parallel either with the [110] or $[1\bar{1}0]$ directions of the substrate. It should be noted that *A* and *C* islands are just mirror images of each other, as are the *B* and *D* islands.

A RHEED pattern taken with the electron beam along the [110] direction of the substrate is reported in Fig. 6. A distinct 2×1 surface superstructure can be recognized (reflections appearing on the circle which is drawn as a guide for the eye) which is associated to uncovered and clean areas of Si(001). 3D transmission spots are also clearly evident (marked by crosses) and correspond to the 3D lattice of $SrF_2(111)$ oriented with the $[11\bar{2}]$ axis along the *e*-beam (parallel to the [110] direction of Si). The position of the fluoride 3D spots relative to the substrate 2D pattern can be accounted for quite accurately if a 7% lattice mismatch between Si and SrF_2 is considered. It is difficult to recognize in the pattern any transmission spots from the other domain of $SrF_2(111)$ rotated by 90°: in principle the associated spots should appear approximately superimposed on the streaks induced by the Si(001) reflections.

B. Electronic properties

Photoemission has been applied to obtain information on bonding between the adsorbed molecules and the substrate at the different growth regimes and to get insights into the interface and subsequent layer composition and stoichiometry. In particular, ultraviolet photoemission was used to probe the evolution of the surface valence band as a function of SrF_2 coverage and substrate temperature. The behavior of the Sr, F, and Si core levels was followed by x-ray photoemission. In the following sections the growth modes at high and low substrate temperature are presented separately.

1. High-temperature growth

a. Sr and F shallow core levels. In Fig. 7(a) the evolution of the shallow core levels of Sr and *F* is reported as a function of SrF_2 nominal coverage when deposition is carried out with the substrate held at 750 °C. The spectra were taken at normal emission (photon incidence angle of 45°) with a photon energy of 90 eV and an overall energy resolution of 0.2 eV. The energy scale is referenced to the Fermi level. The spectra have been normalized to the incoming photon flux.

Only the region below 16 eV of binding energy is shown here. Valence band spectra, measured with He I photons ($h\nu=21.2$ eV) from a discharge lamp, will be discussed in detail in a following section.

The spectrum taken on the clean Si substrate is also reported in the figure. In the energetic interval of interest it is characterized by a featureless, smooth emission. Once SrF_2 molecules are deposited onto the hot surface, a distinct asymmetric structure with a maximum at about 20.4 eV of binding energy shows up. Correspondingly, a weak feature rises at about 39.1 eV. In agreement with results acquired on the $SrF_2/Si(111)$ system,[23] these features (labeled *i*) are associated to interface reacted components of the Sr 4*p* and Sr 4*s* levels, respectively. Similarly to the case of $CaF_2/Si(001)$

(Ref. 4) they are indicative of Sr-Si bonding (in the CaF_2 case, bonding occurs between Ca and Si). It is worth noting that at 0.3 ML of coverage, only the Sr related structures appear: negligible contributions from F atoms can be observed [within the sensitivity of the technique $\leqslant 1\%$; see also the valence band spectra reported in Fig. 11(a) and later discussed]. In analogy to the CaF_2 case, this result is associated with a complete molecular dissociation at the earliest stages of growth. While Sr forms a stable bond with Si, F reevaporates from the surface in the form of volatile compounds with Si. The excess Si atoms needed for this reaction to occur are provided by the consumed substrate terraces, as noted by AFM. A sizeable emission from the F 2*s* states is observed in the spectra only at higher coverage [from 0.8 ML in Fig. 7(a)].

Interestingly, at a coverage of 6 ML the interface related peaks of Sr are still dominant. The pronounced asymmetries of the Sr features towards the high binding energy side of the main peaks are associated to the rising of bulklike components[23] [labeled *b* in Fig. 7(a) at about 22.0 eV for Sr 4*p* and at 40.5 eV for Sr 4*s*]. Concerning the Sr 4*p* levels, the $4p_{1/2}$-$4p_{3/2}$ spin orbit splitting of 1.2 eV (with a branching ratio of 1:2) cannot alone account for the marked asymmetry of the structure. Stemming from the AFM observations which show the development of widely spaced bulklike SrF_2 ridges [Fig. 2(c)], an increase of bulk-related Sr structures is expected. The prevalence of the interface components of Sr levels strongly indicates that the regions in between the islands consist of no more than a few monolayers of SrF_2. This can be easily recognized by considering that the inelastic mean free path for the Sr photoelectrons in a SrF_2 uniform film[24] is below 5 Å.

Concerning the F 2*s* state, it gives rise to a rather broad feature at 0.8 ML of nominal coverage which is centered at 29.9 eV of binding energy. With respect to the expected position for bulk SrF_2, this structure is shifted by about 1 eV towards lower binding energies.[23] This behavior can be ascribed to an interface effect, due both to a change in screening of the core hole caused by the influence of the dielectric constant of the neighboring Si substrate[23,32] and to chemical effects ascribed to the presence of noncompletely dissociated molecules in the form of SrF species.[4] When coverage is increased, the F 2*s* feature slightly shifts and broadens towards the high binding energy side, consistent with the increasing of bulklike contributions.

b. Sr 3*d, F* 1*s and Si* 2*p core levels.* Sr 3*d* levels give rise to intense photoemission peaks when excited with Mg $K\alpha$ radiation. Moreover, Sr 3*d* induced structures have proven in many circumstances to give valuable insights regarding the understanding of chemical reactions and the bonding of Sr atoms or SrF_2 molecules at interfaces with silicon.[25–27] In Fig. 8 the evolution of the Sr 3*d* levels is shown as a function of coverage (expressed in nominal ML) when growth proceeds at a high temperature of 700 °C. The angle integrated spectra were acquired with a double pass CMA operated with an energy resolution of 0.5 eV.

Since the Sr 3*d* peaks appear on a relatively broad plas-

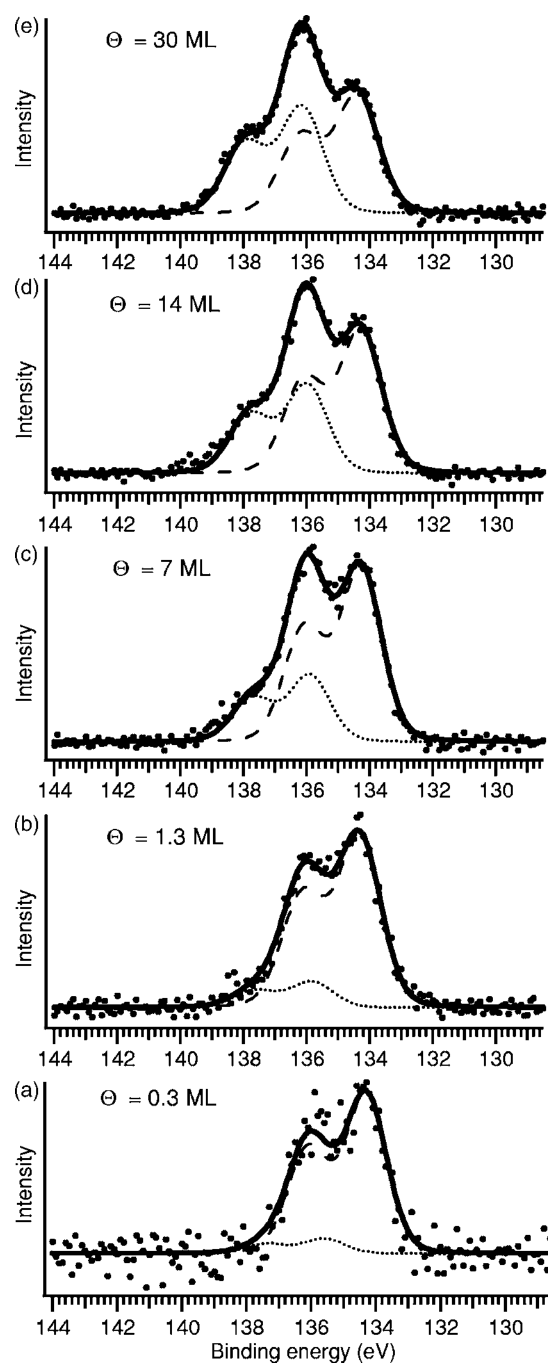

FIG. 8. Sr 3*d* core levels taken at a photon energy of 1253.6 eV (Mg $K\alpha$ line) as a function of coverage after high temperature deposition (700 °C). The spectra were fitted with two Voigt doublets which are associated to bulk and interface reacted SrF_2. Dots represent the experimental points. The broken lines represent the Voigt doublets which result from the curve fitting (continuous line).

mon loss feature of the Si 2*p* emission line, this has been subtracted from the spectra in Fig. 8 before analysis.

The spectra were subsequently decomposed into two Voigt peak doublets, each characterized by a spin orbit splitting of 1.8 eV and a $3d_{3/2}$-$3d_{5/2}$ branching ratio of 0.66. Best fit results were obtained with a common Gaussian full width at half maximum (FWHM) of 1.4 eV and a Lorentzian

FWHM of 0.2 eV for all doublets.

The low binding energy doublet ($3d_{5/2}$ positioned at about 134.5 eV) is associated to interface reacted Sr, while the high binding energy doublet ($3d_{5/2}$ positioned at about 136.0 eV) is ascribed to Sr in a bulklike SrF_2 environment. This assignment is in agreement with previously reported results by Rotenberg *et al.*[26] It can be noticed that at very low coverage [0.3 ML—Fig. 8(a)] the bulk component is negligible and only the interface component contributes to the photoemission peak. Also after the deposition of the first fluoride layer [Fig. 8(b)], the bulk component is still very weak. This finding supports the idea of the formation of a fully reacted wetting layer, in analogy to the CaF_2 case.[4]

The bulk fluoride component increases progressively with increasing coverage, but it never becomes the most prominent feature. On the basis of the considerations which were made in the previous section this can be explained in terms of a reduced effective thickness of the fluoride film (in between the 3D islands) with respect to its nominal value. Interestingly, even at a coverage of 30 ML, the interface reacted component is still well visible and the bulk-related peak accounts only for approximately one half of the total emission.

In order to get more quantitative information on the effective film thickness, the attenuation of the Si 2*p* photoelectron peak was considered (which was measured together with the Sr 3*d* core levels). Assuming that a sharp interface between the fluoride film and the silicon substrate is formed, the effective layer thickness *d* at the various deposition stages can be evaluated to a first approximation according to the relation

$$I = I_o \mathrm{e}^{-\left(\frac{d}{\lambda \cos \theta}\right)},$$

where λ is the inelastic mean free path of the Si 2*p* photoelectrons in the SrF_2 layer, θ is the take-off angle with respect to the surface normal, I_0 and I are the Si 2*p* peak intensities of the bare substrate and after deposition of a layer of SrF_2 of thickness *d*, respectively. Inelastic mean free path values were calculated according to the TPP2M formula.[24] Si 2*p* level intensities were obtained from the area of the related spectra after background subtraction, with $\lambda = 22.9$ Å and an average take off angle $\theta = 44°$ (taking into account the CMA angular acceptance and sample tilt).

In Fig. 9 the effective film thickness obtained with this procedure is plotted as a function of the nominal coverage. It is clearly seen that after the first fluoride layer is deposited, the effective thickness increases very slowly, showing a sort of saturation effect above approximately 15 ML of nominal coverage. As a result, in spite of the large amount of evaporated material, the final SrF_2 film seems to be composed of about 2 atomic layers. This observation is also in agreement with the "anomalous" intensity ratio observed between the interface and bulk photoelectron peaks of Sr, as discussed above. Both these findings are consistent with the idea that the system presents large areas of uncovered wetting layer at the surface with widely separated thick bulklike SrF_2 islands

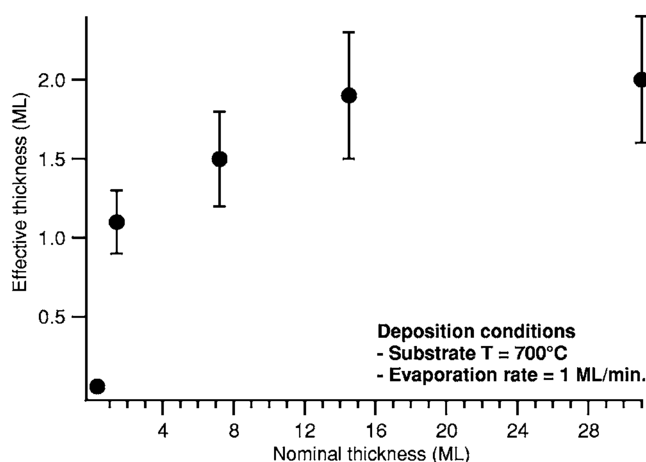

FIG. 9. Effective film thickness as obtained from Sr:F intensity ratios in XPS versus nominal film thickness (quartz thickness monitor readout).

in which the material tends to accumulate, as observed by AFM.

Taking into account the information on the islanding obtained from the AFM results, the relative surface portions of the free interface regions compared to the areas covered by the islands can be estimated from the Sr 3*d* photoemission intensities, considering the appropriate photoelectron sampling depth in each of the two regions and assuming that the 3D islands are so thick that no photoemission intensity is observed from the buried interface below the islands. To this end we used for the Sr 3*d* photoelectrons an inelastic mean free path value of 22.3 Å both for the islands and the interface layer. This corresponds to the theoretical value for SrF_2 at the Sr 3*d* kinetic energy, as derived from the TPP2M formula.[24] An average take-off angle of 44° was also considered. To account for the overall photoemission intensities we consider that while the wetting layer contributes with only a single layer to the interface related signal, in the bulk islands the signal originates from a thicker region and the signal from deeper layers is gradually, exponentially attenuated. That is, deeper layers in the SrF_2 islands contribute progressively less to the bulk related photoemission feature. With this simplified model, we calculate that the area ratios between uncovered/islands regions are approximately 6.7 at 30 ML, 9.7 at 14 ML, and 15.6 at 7 ML. It should be noted that these values are in overall agreement with the surface densities of the islands obtained by AFM and reported above.

XPS is particularly useful also for the evaluation of the stoichiometry of the film as a function of coverage. The composition can be obtained from the intensity ratio of the Sr 3*d* and F 1*s* photoemission peaks, taking into account the relative atomic sensitivity factors (ASF) appropriate to the used electron analyzer.[28] In the present case, the ASF values used were 1.00 for the F 1*s* and 1.05 for the Sr 3*d* peaks, respectively. The Sr:F concentration ratio was evaluated at each evaporation step by measuring the relative peak areas of the Sr 3*d* (including both bulk and interface components) and the F 1*s* photoelectrons after background subtraction and by

dividing by the relative ASF. At very low coverage (0.3 ML) the presence of only Sr at the surface gives a Sr:F ratio equal to 1:0. This indicates complete molecular dissociation occurring at submonolayer coverage and reevaporation of F from the surface in the form of volatile species. At increasing deposition, the fluorine concentration increases, the Sr:F ratio passing from 1:1.4 at 1.3 ML to 1:1.8 at 30 ML (within an accuracy of about 5%). It should be noted that the Sr:F ratio never reaches the molecular stoichiometric value of 1:2. This can be understood in terms of the reduced effective thickness of the fluoride film, as observed above: the first interface layer is enriched in Sr, while most of the material is concentrated into the 3D ridges which present a SrF_2 bulklike composition. The measured concentration ratio is in fact the result of an average over the total amount of Sr and F in the film, within the sampling depth of the technique.

Sr and F photoelectron structures are not sufficient alone to draw conclusions regarding which species form stable bonds with the substrate atoms. To this end, the Si 2p levels have been studied. In order to obtain the higher energy resolution needed to disentangle chemical effects on the Si 2p levels (core level shifts), synchrotron radiation was used. In Fig. 10 Si 2p levels taken at normal emission at a photon energy of 140 eV are reported. The overall energy resolution is 0.3 eV. The spectra are presented after normalization to the incident photon flux, (Shirley) background subtraction and removal of the $2p_{1/2}$ component. This deconvolution procedure does not require any curve fitting. It is only a numerical manipulation of the data, having as inputs the spin orbit splitting (0.6 eV) and the spin orbit ratio (assumed to be the statistical value of 2:1) of the Si $2p_{3/2}$ and $2p_{1/2}$ components. The binding energy scale is referenced to the Fermi level.

The uncovered surface spectrum is reported in Fig. 10(a). A prominent structure is observed at 99.3 eV which is associated to bulk silicon. The silicon dimer-up feature related to the asymmetric dimer reconstruction, which is expected to be observed shifted by about 0.5 eV towards the lower binding energies with respect to the bulk structure,[4,29] is scarcely visible. It contributes to the broad low-binding energy tail of the main peak. The reason for this can be associated to the normal emission condition, which is not the most favorable for the observation of surface induced structures[29] and to the possible presence of defects and contamination at the surface due to nonoptimal heating conditions during the high temperature flashing step to remove the Si oxide layer in the synchrotron run. A broad emission tail is also present at the high binding energy side of the main structure. This is associated both to surface related components[29] of the Si 2p emission and, to a minor extent, to some degree of oxygen contamination.[30] Indeed small traces of oxygen contamination could be observed in wide XPS survey scans. We believe this does not invalidate the major conclusions given below regarding SrF_2 adsorption.

The evolution of the Si $2p_{3/2}$ spectra when SrF_2 is deposited at high temperature (750 °C) is shown in Figs. 10(c) and 10(d). The Si $2p_{3/2}$ structure presents two broad shoulders at high and low energy sides and it is shifted towards higher binding energies with respect to the uncovered silicon surface. To evaluate more quantitatively the different spectral contributions, a fitting of the data was performed. Best fit results were obtained using three Voigt components. They are reported in Fig. 10(c) [analogous results were achieved for the spectrum in Fig. 10(d)]. A common Lorentzian width of 85 meV was used for all components but the Gaussian widths were left to vary independently.

The main contribution at 99.6 eV is assigned to bulk Si. The Gaussian width is 0.4 eV. The binding energy shift of 0.3 eV with respect to the clean surface is consistent to that observed on the CaF_2/Si(001) system under comparable growth conditions.[4] This displacement is related to a band bending caused by the adsorbate, with a shift of the Fermi energy position towards the Si conduction-band edge. This behavior is also analogous to what is observed on alkali metal covered Si(001) surfaces[31] and can be related to the birth of unoccupied adsorbate-induced states.[21,32]

The low binding energy structure at 99.2 eV (Gaussian width 0.5 eV) is attributed to Si bonded to Sr at the interface. The energy shift between the bulk peak and the Sr-related component is 0.4 eV, which is only slightly smaller than the value of 0.5 eV reported for Sr adsorption on Si(001).[25] This is perfectly consistent with values found for SrF_2 adsorption on Si(111) (Ref. 23) and can be related to the fact that Sr bonding to Si substrate atoms originates both from completely dissociated molecules and from partially dissociated SrF species through Si-SrF bonding, in analogy to the CaF_2/Si(001) case.[4] The two different contributions may be too close in energy to be resolved and may account for the width and position of the Sr-related peak.

The high binding energy structure is centered at 100.15 eV and is broader than the two former structures. Its shift with respect to the bulk peak is 0.55 eV. The assignation is not straightforward, since Si-F related structures which are known to contribute to the high binding energy side of the Si 2p levels are expected to show up with a shift of about 1 eV (for SiF_1).[33] One possibility is associating it to bonding of Si with partially dissociated SrF molecules in the form of Si-F-Sr complexes, leading to a reduced interaction between the Si atoms and the (SrF) ions with respect to the F ions alone. The significantly large Gaussian width of about 0.95 eV can be related to both a certain degree of disorder in the interface region or to different components that we are unable to resolve. In this respect, the high binding energy tail of the F related structure can indeed include SiF_1 shifted components. On the other hand, the presence of surface defects due to the lattice mismatch can also account for the high binding energy shoulder, resulting in enhanced inelastic scattering of the electrons from the main Si peak as they pass through the interface layer.

The association of the 0.55 eV shifted structure only to oxidized species seems improbable, both because the pronounced intensity of the structure is inconsistent with the small traces of oxygen revealed by XPS with respect to fluorine and because shifts of the order of 1 eV or higher[30] are

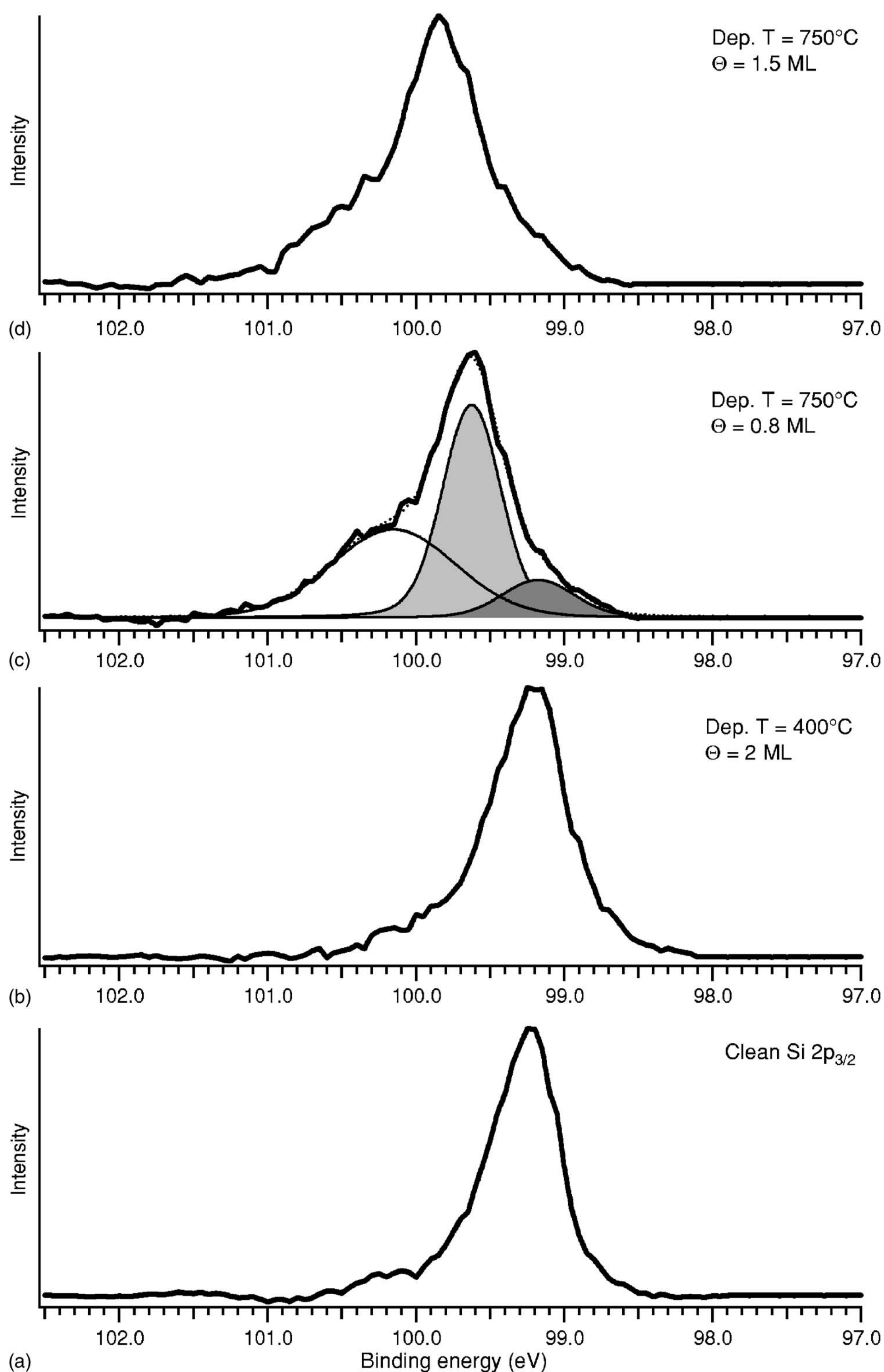

FIG. 10. Si $2p_{3/2}$ photoemission peak measured at normal emission at a photon energy of 140 eV; panel (a) refers to the clean Si surface, (b) refers to 2 ML of SrF_2 deposited at 400 °C, (c) and (d) refer to 0.8 ML and 1.5 ML respectively, deposited at 750 °C. The spectrum of Fig. 10(c) has been decomposed into three Voigt profiles.

expected for oxidized components. Moreover, it is expected that whenever present, incorporated oxygen should be removed upon annealing to 700 °C,[21] which is below the growth temperature applied here.

c. Valence band. Valence band spectra were taken with a conventional UV discharge source, operated with 21.2 eV photons. In Fig. 11(a) the experimental electron distribution curves corresponding to different nominal thicknesses of SrF_2 grown at high temperature (700 °C) are reported. Spectra are angle integrated, as they have been acquired with a double-pass CMA with an energy resolution of 0.1 eV. The topmost region of the valence band down to about 5 eV of binding energy is shown in greater detail in the inset of the figure. The clean surface spectrum is also reported for comparison.

The clean surface presents distinct features that correspond to emission from surface states at about 0.8 eV of binding energy and other structures at higher energy in

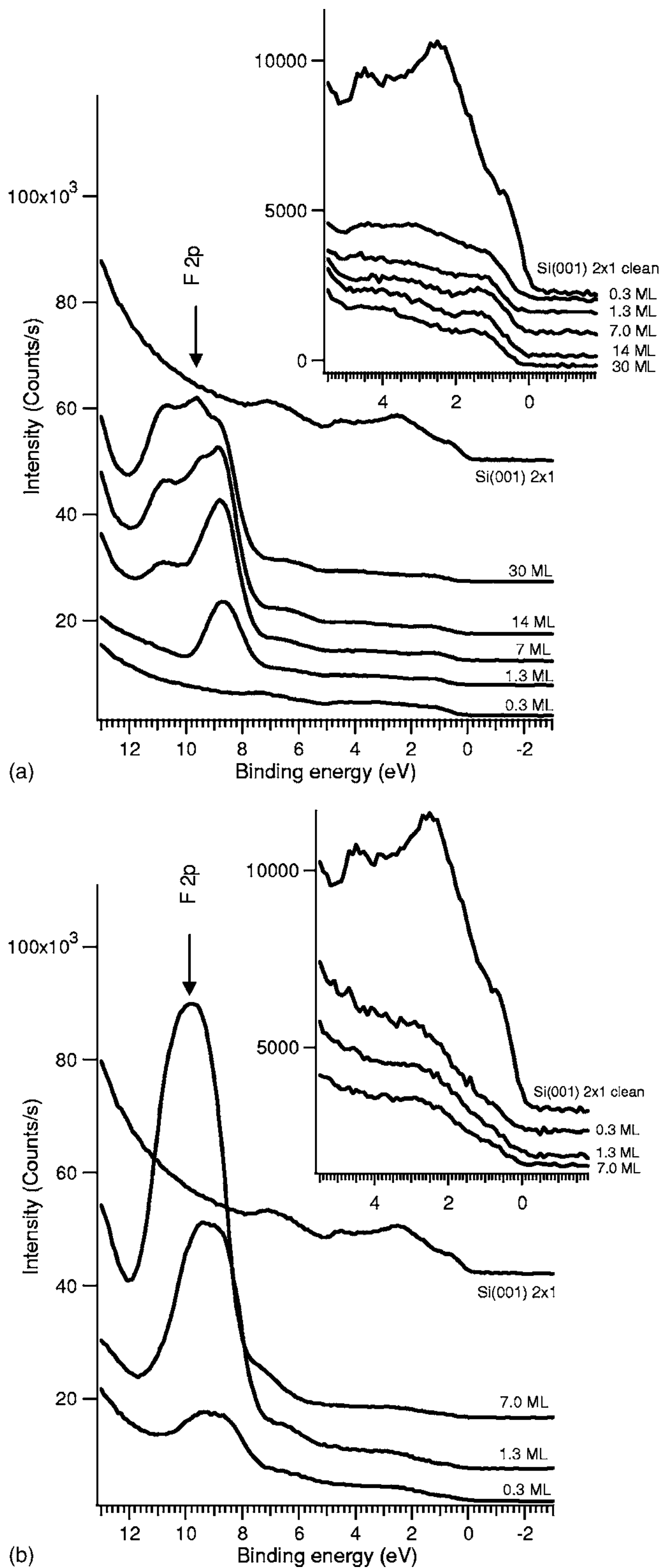

FIG. 11. Angle integrated ultraviolet photoemission spectra taken at 21.2 eV of photon energy after deposition at (a) high and (b) low temperature as a function of coverage. The valence band top is shown in greater detail in the insets. For visualization purposes the spectra have been shifted on the vertical scale with respect to each other.

agreement with literature results.[34] From the initial deposition stages at high temperature, at sub-monolayer coverage [Fig. 11(a)], the features of the clean Si surface are severely damped. A distinct feature, which can be ascribed to emission from the F 2p valence band appears at about 1 ML of coverage, centered at 8.6 eV of binding energy. This feature evolves with coverage, first with the emergence of a pronounced shoulder at 10.8 eV, then with the development of a more complex structure between 8 and 12 eV. While the narrow F 2p structure observed at low coverage can be associated with an interface-reacted fluoride layer, the large structure observed at high coverage is associated with the development of the bulklike F 2p valence band of SrF_2, similarly to the case of CaF_2/Si(001).[2,3]

It is worth noting that the spectrum taken at 0.3 ML of coverage does not show any signal related to the fluorine valence band. This is consistent with the core levels' behavior illustrated above and it is connected to complete molecular dissociation, leading to Sr bonding to Si. In relation to this, a new feature is observed at about 1.5 eV of binding energy [inset of Fig. 11(a)], which can be associated to the Sr 5s state of the dissociated interface layer.[23] This structure shows its maximum intensity after the development of the wetting layer and then slightly reduces with coverage. This is consistent with the fact that large areas of the reacted interface layer are left uncovered by the SrF_2 3D ridges even at the highest nominal coverage investigated [Fig. 2(c)].

Concerning the presence of the Sr 5s state, the interface behaves in complete analogy with the CaF_2/Si case[2,3,32] grown at high temperature, where interface states related to the Ca 4s electrons in the reacted layer are clearly identified. Moreover, this result is also in agreement with the observations by Olmstead *et al.* for the dissociative SrF_2 chemisorption on Si(111) at high temperature.[23]

A final consideration is due to the low binding energy onset of the spectra. It can be noticed [inset of Fig. 11(a)] that the emission onset shifts towards lower binding energy with respect to the Fermi level when SrF_2 is deposited onto Si at high temperature. This is consistent with the downward shift of the Si 2p bulk-related feature observed in Figs. 10(c) and 10(d). The magnitude of the shift can be evaluated by extrapolating the onset of the valence band top with a straight line. A value of −0.3 eV is obtained, which is in perfect agreement with the Si 2p level behavior (see above) and relates to a band bending induced by the interface with a concomitant shift of the Fermi level closer to the bottom of the conduction band.

Similarly the F 2p position permits us to evaluate the valence band offset at the SrF_2/Si interface, which is directly related to the interface dipole and to the F concentration in the wetting layer.[35] Extrapolating the onset of the F 2p feature with a straight line a value of about 7.0 eV is obtained, which is sizably lower than the corresponding value of about 8 eV obtained for SrF_2/Si(111) (Ref. 23) and CaF_2/Si.[2,3,21] According to Satpathy and Martin,[35] a reduced valence band offset is related to an increased amount of F atoms at the interface which reduce the charge transfer to the Si atoms

and decrease the dipole strength. This is not in contrast with our findings from the core levels, which suggest the presence of possible Si-F bonding.

2. Low-temperature growth

a. Sr and F shallow core levels. The evolution of the F 2*s* and Sr 4*p* and 4*s* shallow levels as a function of coverage is reported in Fig. 7(b), when deposition is carried out at 400 °C. In analogy to Fig. 7(a), the background emission of the clean substrate is also shown in the energy region of interest.

Differently from the high temperature growth case, at low temperature F- and Sr-induced structures appear in the spectrum already at very low deposition stages (0.5 ML). During high-temperature growth, all structures were mainly ascribed to emission from interface reacted molecules. At low temperature both Sr and F features appear shifted towards higher binding energy and this suggests associating them to emission from SrF_2 in a bulklike environment.[23] In particular, Sr 4*p* states are centered at 22.0 eV of binding energy, F 2*s* at 31.0 eV and Sr 4*s* at 40.5 eV. The observation of bulk-related fluoride structures is not unexpected, and it is to be related to the development of the 3D fluoride triangular islands, as shown by AFM.

Interestingly, at submonolayer coverage all peaks appear shifted towards lower binding energies, a situation which resembles the high temperature growth. Although less visible for F 2*s* and Sr 4*s* states, the shifted component determines a sizeable shoulder at the low binding energy side of the Sr 4*p* emission even at higher coverage. Consistent with the high temperature case, this is associated with an interface effect [labeled by *i* in Fig. 7(b)]. The presence of this type of feature seems to suggest that even at low temperature a certain degree of molecular dissociation is present at the interface with silicon. In this respect, the system seems to behave differently from the CaF_2/Si(001) case,[4] where no clear traces of a strong interaction with the substrate were identified at a comparable deposition temperature. The result shown here is consistent with reports by Olmstead,[21] indicating that molecular dissociation is already active when deposition is carried out at 400 °C on Si(111) surfaces.

Associating the shifted components to surface fluoride features seems unlikely, since it was observed[21] that surface-related emission tends to contribute mainly towards the high binding energy side of the cation states.

b. Sr 3d, F 1s and Si 2p core levels. Sr 3*d* core levels are shown in Fig. 12. Spectra were taken under the same experimental conditions as the data reported in Fig. 8 and the same data reduction procedure (background subtraction and data fitting) was applied.

When growth proceeds at low substrate temperature, the Sr 3*d* spectra appear broader and less resolved with respect to the high temperature case. In particular, all spectra were fitted with a unique Voigt doublet component ($3d_{5/2}$ positioned at about 135.0 eV for all spectra). In this case, best fit results were obtained with a common Gaussian FWHM of 1.8 eV and a Lorentzian FWHM of 0.3 eV. Attempts to use

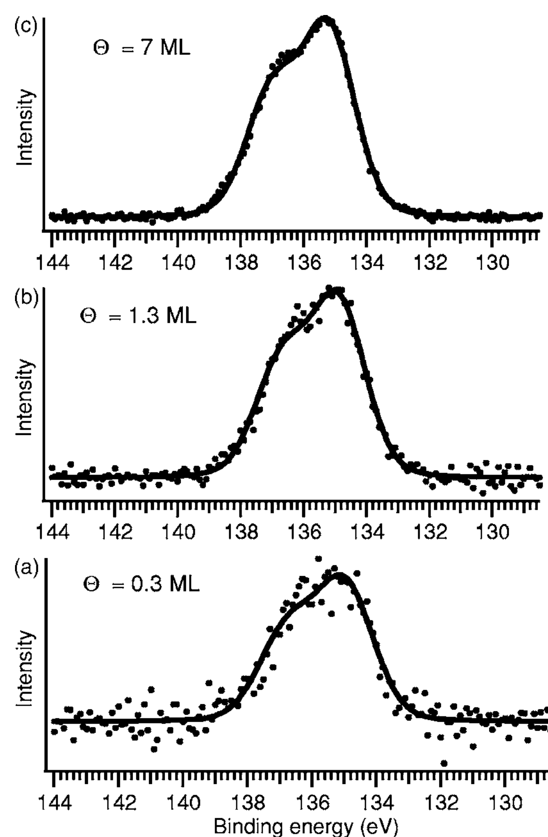

FIG. 12. Sr 3*d* core levels taken at a photon energy of 1253.6 eV (Mg $K\alpha$ line) as a function of coverage after low temperature deposition (400 °C). The spectra were fitted with a single Voigt doublet, as shown by the continuous line. Dots are the experimental points.

two distinct Voigt doublets of the same type and energy positions of the high temperature case did not produce valid fitting results.

The broadening of the Sr 3*d* line with respect to the high temperature case can be interpreted in terms of multiple components which cannot be well separated within the energy resolution available and possibly to a certain degree of disorder. Correlating with the behavior of the shallow core levels, it can be assumed that the contributions to the Sr 3*d* spectra originate mainly from SrF_2 in a bulklike environment and from partially dissociated molecules in the form of SrF complexes, possibly not strongly interacting with the substrate. Contributions from totally dissociated molecules resulting in the bonding of atomic Sr to Si seem to be excluded at low temperature.

Following the same scheme applied at high temperature, XPS was used to give an estimation of the nanostructured film stoichiometry at increasing coverage steps. The relative concentrations of Sr and F are independent on thickness, with a Sr:F ratio equal to 1:2 (the molecular stoichiometric value, within an accuracy of approximately 5%) at all investigated coverages. This further supports the idea that if some degree of molecular dissociation is present at the interface, no sizeable F loss from the system occurs in the form of volatile species, in contrast to the situation which is encoun-

tered at high temperature.

In Fig. 10(b), the Si $2p_{3/2}$ level is shown after growth of 2 ML of SrF_2 at low substrate temperature. It can be seen that SrF_2 adsorption at low temperature does not produce significant variation in the Si $2p$ line shape with respect to the bare Si surface [Fig. 10(a)]. This can be interpreted in terms of no strong interaction of the molecules with the substrate, in contrast to high temperature deposition. This situation is analogous to that observed on CaF_2/Si(001).[4]

c. Valence band. Angle integrated spectra of the valence band of the nano-structured SrF_2 film grown at low temperature are reported in Fig. 11(b). The inset shows in greater detail the region below 5 eV of binding energy, where Si surface states and Sr induced states are expected to give contributions.

From the earliest stages of evaporation, the F $2p$ valence band is present in the spectra, consistent with the fact that at a not high enough temperature, F does not leave the surface, differently from the high temperature case. The F $2p$ band gives rise to a broad, unstructured feature which initially is centered at about 9.2 eV of binding energy, then slightly shifts towards higher binding energy (9.9 eV at 7 ML). This behavior is in agreement with the evolution of the shallow core levels discussed above.

The line-shape of the F $2p$ feature differs significantly from the experimentally derived band typical of bulk SrF_2.[23] In particular it does not present the characteristic fine structure which is also partly observed in the present study at high coverage during high temperature growth and which is associated to the formation of the bulk crystal phase. Instead, the smooth line-shape presents strong similarities to that observed for CaF_2 growth on Si(001) at low temperature[2,3] and which was ascribed to the F $2p$ valence band of nanodimensional fluoride islands. In the present case, also considering the core level results, it seems reasonable to associate the observed broad feature both to the reduced dimensionality of the fluoride islands and to some degree of dissociated molecules, contributing mainly to the low binding energy side of the F $2p$ emission.

The valence band offset, evaluated by extrapolating the emission onsets on the spectra with straight lines, gives a value of 7.2 eV, which is only slightly higher that the value obtained during high temperature growth, but still it is significantly lower than the values reported for CaF_2[21] and for SrF_2 films on Si(111).[23]

Concerning the silicon valence band top, no clear contributions are observed from Sr-induced states [inset of Fig. 11(b)]. Instead, the spectral evolution shows mainly a progressive damping of all structures related to the silicon surface. This result is in agreement with the idea that the part of the surface which is not covered by the SrF_2 nanoislands remains bare Si(001). Again an analogous behavior was observed for CaF_2.[2,3]

C. Comparison with the CaF_2/Si(001) interface

The present work extends a previous study[2–4] dedicated to the growth on Si(001) of nanostructured fluoride films with cubic lattices. Two quite distinct growth regimes are identified. One gives rise to SrF_2 (110) ridges on top of the reacted interface layer when deposition is carried out at high substrate temperature of the order of 700–750 °C. The other gives rise to three-dimensional SrF_2 (111) islands which leave portions of the Si surface uncovered and unreacted when deposition is carried out at low substrate temperatures below 500 °C.

Concerning high temperature growth, the system presents strong similarities with CaF_2/Si(001). In both cases a wetting layer is formed with the preferential consumption of A-type terraces with respect to B-type ones [Fig. 1(b)]. We believe this is associated to the crucial role played by the step edges on the molecular dissociation and reaction with the Si substrate atoms and in particular to the different reactivity of S_A and S_B type steps. The similarity of the spectroscopic and structural results obtained for CaF_2/Si(001) and SrF_2/Si(001) at monolayer and submonolayer coverage indicates that the principal interfacial bonding is dominated by chemical driving forces, which seem to be not much influenced by the value of the lattice mismatch. This gives rise in both cases to a 3×1 single domain surface reconstruction. Although the elementary mechanisms which induce the molecular interaction with the substrate and dynamics of the wetting layer formation are analogous for both SrF_2 and CaF_2, the high lattice mismatch between the SrF_2 and Si lattice is believed to be responsible for some degree of disorder at the interface with respect to CaF_2. This effect is expected to be further enhanced during the growth of subsequent layers on top of the first reacted wetting layer because of the large strain induced in the film. This can explain both the appearance of long range periodicity in LEED and RHEED patterns once coverage exceeds the first layer and the possible direct interaction between Si and F, which is suggested by photoemission, with the formation of SrF-Si complexes and F-Si bonding due to residual F atoms which are not reevaporated from the surface and are incorporated into the interface layer.

At low deposition temperatures the growth modes of CaF_2 and SrF_2 differs substantially. While in the first case rectangular based crystalline fluoride islands develop which are oriented with their CaF_2[001] axis parallel to the Si[001] axis,[4] in the second case SrF_2 grows forming triangular based islands which present their SrF_2[111] axis perpendicular to the surface plane. A common feature is the persistence of bare Si(001) surface areas in between the developing fluoride nanostructures, at least when coverage is not high enough to induce complete coalescence of the islands.

This discrepancy can be explained in terms of the large lattice mismatch between SrF_2 and Si compared to CaF_2. In this respect the chemical interaction between molecules and substrate atoms does not seem sufficient to determine the final film morphology. This is mainly due to the lattice parameter of the growing fluoride. A good matching, as for CaF_2, induces a growth mode in registry with the substrate. A poor matching causes the fluoride crystal to grow along its [111] direction, which lowers the surface free energy of the system. Chemical interactions (weaker than in the high temperature case) between the buried interface molecules and

substrate, are not sufficient to overcome the driving forces guiding the growth of SrF_2 bulklike crystallites. Concerning the islands' nucleation sites, it was noted that SrF_2 nanostructures nucleate preferentially at step edges, inducing an anisotropic decoration of the surface [Fig. 5(a)]. At a temperature of 400 °C adsorbed molecules are sufficiently mobile at the surface and nucleation sites occur preferentially at step edges where mobility is reduced due to the step barrier.

An interesting point regards molecular reaction and dissociation at low temperature deposition. The appearance of interface reacted components in photoemission spectra of Sr $4p$, Sr $4s$, F $2s$ levels [Fig. 7(b)] and the broad emission from Sr $3d$ states (Fig. 12) which is ascribed to the presence of different types of emitting sites (bulklike as well as interface related Sr atoms) seem to suggest that some degree of molecular dissociation is present at low temperature. This is consistent with observations by Olmstead[21] on the CaF_2/Si(111) system. On the other hand the SrF_2 molecular stoichiometry is always preserved for low temperature growth even at very low coverage, as measured by XPS. This seems to indicate that, in the case of molecular dissociation, the extra F atoms do not leave the surface as in the high temperature growth mode and tend to remain trapped at the interface. It is noteworthy that inspection of Si $2p$ core levels gives no clear indication of bonding between the substrate Si atoms and F or Sr species. It is possible that some reacted component is actually masked by the peak amplitudes in the present experiment and cannot be resolved. Nevertheless a completely similar result was obtained for CaF_2 deposition on Si(001) at the same temperature.[4] The question of the location of the excess F atoms and the details of the interface reaction between Si and SrF_2 molecules during low temperature growth (400 °C) remains open and deserves further investigation.

IV. CONCLUSIONS

The growth mode of SrF_2 on Si(001) has been studied following a multitechnique approach which includes the application of structural as well as electronic properties probes. In particular AFM, RHEED, and LEED were used to determine film morphology and crystal properties as a function of thickness and substrate temperature during deposition. Photoemission in the soft-X and in the ultraviolet photon range were applied to get insights into molecular reaction and bonding with the substrate. This work continues and extends a preceding analogous study regarding the growth of CaF_2 on Si(001). One main objective was to investigate the role of the lattice parameter in the determination of the final film properties of cubic fluorides on Si(001).

In analogy to the CaF_2 case two distinct growth regimes are identified. At a deposition temperature around 400 °C flat triangular SrF_2 islands are formed on the surface which are aligned with their [111] crystal axis perpendicular to the surface plane. At high deposition temperatures (700–750 °C), molecular dissociation and reaction with the substrate atoms leads to the formation of a wetting layer which covers the substrate uniformly and presents a 3×1 uniaxial periodicity. The reason for this is associated to the preferential and selective dissociative reaction of the fluoride molecules at substrate step edges which are aligned perpendicular to the Si dimer rows of the upper terrace (S_B-type of steps), with the reevaporation of the excess F atoms in the form of volatile species with Si. On top of the wetting layer, SrF_2 growth proceeds with the formation of large islands having the shape of ridges facetted with {111} planes. The effective film thickness evaluated by photoemission suggests that in the area between the ridges SrF_2 does not grow on top of the interface layer. Electron diffraction techniques indicate the presence of some interface disorder (or rather long range periodicity) which is to be ascribed to the large mismatch between the Si and SrF_2 lattices.

ACKNOWLEDGMENTS

This work has been supported by AREA Trieste under research project No. 4, N188 and by the Russian Ministry of Education and Science (Contract No. 2006-RI-112.0/001/034). The experiments at the BEAR beam line at ELETTRA have been carried out under proposals 2003665 and 2004219. The authors of the paper are grateful to the BEAR beam line, M. Montecchi and A. S. Balanev for assistance during the synchrotron measurements.

[1] N. S. Sokolov, S. M. Suturin, V. P. Ulin, L. Pasquali, G. Selvaggi, and S. Nannarone, Appl. Surf. Sci. **234**, 480 (2004).
[2] L. Pasquali, S. D-Addato, G. Selvaggi, S. Nannarone, N. S. Sokolov, S. M. Suturin, and H. Zogg, Nanotechnology **12**, 403 (2001).
[3] L. Pasquali, S. Suturin, N. Sokolov, G. Selvaggi, S. D'Addato, and S. Nannarone, Nucl. Instrum. Methods Phys. Res. B **193**, 474 (2002).
[4] L. Pasquali, S. M. Suturin, V. P. Ulin, N. S. Sokolov, G. Selvaggi, A. Giglia, N. Mahne, M. Pedio, and S. Nannarone, Phys. Rev. B **72**, 045448 (2005).
[5] D. J. Chadi, Phys. Rev. Lett. **59**, 1691 (1987).
[6] T. Chatterjee, P. J. McCann, X. M. Fang, and M. B. Johnson, J. Vac. Sci. Technol. B **16**, 1463 (1998).
[7] M. Watanabe, I. Iketani, and M. Asada, Jpn. J. Appl. Phys., Part 2 **39**, L964 (2000).
[8] K. Mori, W. Saitoh, T. Suemasu, Y. Kohno, M. Watanabe, and M. Asada, Physica B **227**, 213 (1996).
[9] S. Nannarone, F. Borgatti, A. DeLuisa, B. P. Doyle, G. C. Gazzadi, A. Giglia, P. Finetti, N. Mahne, L. Pasquali, M. Pedio, G. Selvaggi, G. Naletto, M. G. Pelizzo, and G. Tondello, AIP Conf. Proc. **705**, 450 (2004).
[10] R. F. C. Farrow, P. W. Sullivan, G. M. Williams, G. R. Jones, and D. C. Cameron, J. Vac. Sci. Technol. **19**, 415 (1981).
[11] A. Ishizaka and Y. Shiraki, J. Electrochem. Soc. **133**, 666 (1986).
[12] M. Reichling, M. Huisinga, D. Ochs, and V. Kempter, Surf. Sci.

402-404, 145 (1998).

[13] Mean radius 66 mm, made by the *Gruppo Progettazione Strumentazione* of INFM, UdR Roma3, G. Paolicelli, A. Fondacaro, and G. Stefani.

[14] See for example: G. V. Hansson and R. I. G. Uhrberg, Surf. Sci. Rep. **9**, 197 (1988); A. Ramstad, G. Brocks, and P. J. Kelly, Phys. Rev. B **51**, 14504 (1995).

[15] D. J. Chadi, Phys. Rev. Lett. **59**, 1691 (1987).

[16] H. Okada, Y. Fujimoto, K. Endo, K. Hirose, and Y. Mori, Phys. Rev. B **63**, 195324 (2001).

[17] T. Yokoyama and K. Takayanagi, Phys. Rev. B **57**, R4226 (1998).

[18] T. Komura, T. Yao, and M. Yoshimura, Phys. Rev. B **56**, 3579 (1997).

[19] J. Wang, J. A. Hallmark, D. S. Marshall, W. J. Ooms, P. Ordejón, J. Junquera, D. Sánchez-Portal, E. Artacho, and J. M. Soler, Phys. Rev. B **60**, 4968 (1999).

[20] V. A. Ukraintsev, Z. Dohnálek, and J. T. Yates Jr., Surf. Sci. **388**, 132 (1997).

[21] M. A. Olmstead, in *Thin films: heteroepitaxial systems*, edited by W. K. Liu and M. B. Santos (World Scientific, Singapore 1999).

[22] S. M. Suturin *et al.*, to be published.

[23] M. A. Olmstead and R. D. Bringans, Phys. Rev. B **41**, 8420 (1990).

[24] The inelastic electron mean free path can be calculated from the Tanuma, Powell, and Penn TPP2M formula: S. Tanuma, C. J. Powell, and D. R. Penn, Surf. Interface Anal. **21**, 165 (1993).

[25] A. Herrera-Gómez, F. S. Aguirre-Tostado, Y. Sun, P. Pianetta, Z. Yu, D. Marshall, R. Droopad, and W. E. Spicer, J. Appl. Phys. **90**, 6070 (2001).

[26] E. Rotenberg, J. D. Denlinger, M. Leskovar, U. Hessinger, and M. A. Olmstead, Phys. Rev. B **50**, 11052 (1994).

[27] E. Rotenberg, J. D. Denlinger, and M. A. Olmstead, Phys. Rev. B **53**, 1584 (1996).

[28] G. E. Mulienberg, in *Handbook of X-ray photoelectron spectroscopy*, (Norvalk, Physical Electronics Div., Perkin Elmer Corp., 1979).

[29] E. Landemark, C. J. Karlsson, Y.-C. Chao, and R. I. G. Uhrberg, Phys. Rev. Lett. **69**, 1588 (1992).

[30] F. J. Himpsel, F. R. McFeely, A. Taleb-Ibrahimi, J. A. Yarmoff, and G. Hollinger, Phys. Rev. B **38**, 6084 (1988).

[31] Y.-C. Chao, L. S. O. Johansson, and R. I. G. Uhrberg, Phys. Rev. B **55**, 7198 (1997).

[32] D. Rieger, F. J. Himpsel, U. O. Karlsson, F. R. McFeely, J. F. Morar, and J. A. Yarmoff, Phys. Rev. B **34**, 7295 (1986).

[33] F. R. McFeely, J. F. Morar, N. D. Shinn, G. Landgren, and F. J. Himpsel, Phys. Rev. B **30**, 764 (1984); J. F. Morar, F. R. McFeely, N. D. Shinn, G. Landgren, and F. J. Himpsel, Appl. Phys. Lett. **45**, 174 (1984).

[34] R. D. Bringans, R. I. G. Uhrberg, M. A. Olmstead, and R. Z. Bachrach, Phys. Rev. B **34**, 7447 (1986); F. J. Himpsel and D. E. Eastman, J. Vac. Sci. Technol. **16**, 1297 (1979).

[35] S. Satpathy and R. M. Martin, Phys. Rev. B **39**, 8494 (1989).